NOTICE CONCERNING COPYRIGHT RESTRICTIONS

PERFORMANCE MATCHING AND PREDICTION FOR SERRAZZANO GEOTHERMAL RESERVOIR BY MEANS OF NUMERICAL SIMULATION

K. Pruess, O. Weres, R. Schroeder, R. Marconcini, and G. Neri

1. Introduction

Serrazzano geothermal reservoir is one of the distinct zones of the extensive geothermal area near Larderello in central Tuscany, Italy. Natural manifestations and utilization of steam and hot water from shallow holes in this region have occurred for centuries. Deep drilling was begun after 1930, and since 1939 electric power has been generated at Serrazzano from geothermal steam (with an interruption in World War II, when the wells were destroyed).

We have developed a distributed-parameter history-match simulation of the performance of Serrazzano reservoir from 1959 to 1975. The reservoir model obtained from this was subsequently used for predicting the future performance of Serrazzano reservoir through 1990. To our knowledge, no such simulation has ever been attempted for a producing vapor-dominated geothermal reservoir. Serrazzano was chosen as a case study for developing and evaluating the methodology for two reasons: (1) detailed production data and much geological and hydrological information is available for the reservoir; (2) for environmental reasons surface disposal of produced brines is no longer acceptable in Italy, and numerical studies are needed to aid in developing an appropriate injection program.

The numerical simulations presented in the present paper were carried out with a computer program called SHAFT79. This program was developed at Lawrence Berkeley Laboratory, and is briefly reviewed in Chapter 2. Data base and elements of a conceptual model for Serrazzano are discussed in Chapter 3. Subsequently we explain the method used in developing a history

match simulation, and present results for our current "best" model of Serrazzano reservoir. Several effects which could cause a more rapid reservoir decline are examined in Chapter 6, and Chapter 7 presents the extrapolation of reservoir performance through 1990.

2. The Simulator SHAFT79

SHAFT79 solves coupled mass- and energy-transport equations for two-phase flow in a porous medium, using an integrated finite difference method. This method allows a very flexible one-, two-, or three-dimensional description of reservoirs, and is easily applicable to irregular shapes and geological features. Methodology and applications of SHAFT79 have been discussed in

of Serrazzano geothermal reservoir on LBL's CDC-7600 computer.

3. The Data Base

At the present time, Serrazzano field has 19 producing wells and 18 wells which are shut in because they are dry or nearly dry. The produced fluid is

simulated time	number of time steps	average time step	total CPU-time	CPU-time per time step	typical throughput
15.5 years	243	23.3 days	2267 sec	9.3 sec	12.7

Table 1: SHAFT79 - Performance for Serrazzano Simulation. Throughput is the ratio of mass produced in a time step to mass initially in place in the producing element (the figure given is for well Pozzaie 2 at element N4, see Figure 1).

approximately 96.5% superheated steam, and 3.5% non-condensable gases (mainly CO_2). Liquid water has never been encountered at Serrazzano. However, mass balance considerations demonstrate convincingly that most of the fluid reserves in Serrazzano are in place in liquid form.[8] From the drill logs it has been possible to identify the permeable strata of the reservoir, and to map the geometry of the system.[9,10] The reservoir is an anticlinal horst-and-graben structure, with thickness varying from some ten meters near the intensely fractured structural high to more than 500 meters in areas with thick layers of "evaporite" rocks (see Figure 1). The "evaporite" complex consists of highly permeable and porous anhydrite, limestones, and radiolarites. The location of impermeable boundaries is somewhat open to question.

Formations underlying the structural high may have non-negligible permeability and porosity. Fractures are known to play an important role in fluid transport in Serrazzano.[11,12] It appears possible that significant amounts of steam are brought through fractures into the main reservoir from great depth (> 2 km).

Geochemical and hydrological work has shown that Serrazzano field is a rather isolated section of the Larderello geothermal region; no significant recharge is believed to occur.[13]

Average properties of the rock matrix are subject to large uncertainty. Laboratory tests on cuttings have given consistent values for specific density, specific heat, and heat conductivity. However, average porosity and permeability cannot be determined from core samples on a laboratory scale. These parameters are very poorly known. A few drawdown- and buildup-tests have been conducted in the past, from which a rough picture of the kH-distribution has been inferred.[14,15] Interpretation of these tests is questionable due to 2-phase conditions in parts of the reservoir.

Wellhead temperature and pressure measurements in flowing wells, and pressure measurements in shut-in wells, provide a basis for determining average thermodynamic conditions in the reservoir. Interpretation of these data is complicated by substantial variations on a local scale, sometimes due to deep fractures, sometimes due to shallow cold aquifers.

Operating conditions in Serrazzano approximate production with constant pressure p = 5 bars. Many wells have rather small flow rates, and estimation of downhole conditions is uncertain because of unknown and possibly large effects from heat losses to shallow aquifers.[8]

Important work on average pressure distributions in Serrazzano was done by Atkinson et al. (ref. 16). Using somewhat subjective judgment in evaluating field data with their sometimes large fluctuations and local variations, these authors were able to construct several contour maps of average reservoir pressures between 1960 and 1975. These pressure maps, when combined with temperature data, show that superheated conditions prevail throughout the main well field, near the structural high.

No direct information exists regarding the distribution of pore water in the reservoir. A rough hint is available from a conceptual model of Serrazzano as developed by Weres et al.[17,18] Postulating hydraulic continuity with surrounding aquifers, and using a plausible value of T = 275°C for initial (pre-exploitation) reservoir temperature at depth, the steam/two-phase interface is estimated near 500 m depth.

Positions, producing horizons, and time-dependent flow rates are known for all wells.

In summary: Although much data and qualitative information is available for Serrazzano, the data base falls very much short of the detailed and

complete definition required as input for distributed parameter simulation. Moreover, available data reflect actual field conditions to varying degrees, and are subject to various degrees of confidence. As indicated in Table 2, the most significant deficits with regard to data availability exist in the areas of permeability, distribution of pore water, and porosity. Partially unavailable or uncertain are data defining geometry and boundary conditions of the reservoir, and the detailed distribution of temperatures and pressures.

4. Method of Simulation

The simulation is carried out using the geologically accurate mesh as developed by Weres (ref. 18,19). Figure 1 gives an areal view of the reservoir, with the positions of the geological cross-sections employed in the mesh generation indicated by straight lines labeled A to Z. Figure 2 shows the computer-generated mesh in two different (rotated) views. The mesh represents a reservoir that is a curved thin sheet approximately 1 km from top to bottom, and areally covers about 25 km^2. It has 234 polyhedral elements with 679 polygonal interfaces between them. There are up to 10 interfaces per element.

Our initial attempts to model the pre-exploitation phase were soon abandoned when it became apparent that the almost complete lack of data would leave us with a multitude of rather meaningless parameter choices. Subsequently, we endeavored to model the post-1959 period, for which rather detailed field data are available.

The data (Table 2) have to be grouped into those which are provided as input to the simulation, and those against which simulated results are compared. The division between the two groups is to some extent arbitrary. We noted before that operating conditions in Serrazzano approximate production with

PARAMETERS	RATING Availability	Sensitivity	HANDLING
geometrical definition of reservoir	A-B	β	Essentially fixed (minor adjustments where imperative)
rock properties: density ρ ; specific heat C_R; heat conductivity K_R	A	α	fixed (ρ = 2600 kg/m^3; C_R = 775 J/kg^oC; K_R = 2.1 W/m^oC)
permeability: k	B	β	adjustable
porosity: ϕ	B	α	fixed at somewhat arbitrary ϕ = 10%
boundary conditions	A-B	α-β	fixed (no flow)
initial conditions: temperature T; pressure p;	A-B	β	adjustable within a range
vapor saturation S	B	β	adjustable
wells: locations	A	β	fixed } as measured
flow rates	A	β	fixed } as measured
pressures p as function of time	A-B	-	to be matched by simulation

Table 2: Serrazzano Data Base. The various parameter groups needed for a simulation are rated on scales of availability (A: rather good definition from field data; B: not well defined from field data, hence susceptible to rather arbitrary adjustments; A-B: intermediate) and sensitivity (α: parameter variations have little impact on simulated field performance; β: parameter variations have strong impact on simulated field performance; α-β: intermediate). Availability ratings apply to period after 1960.

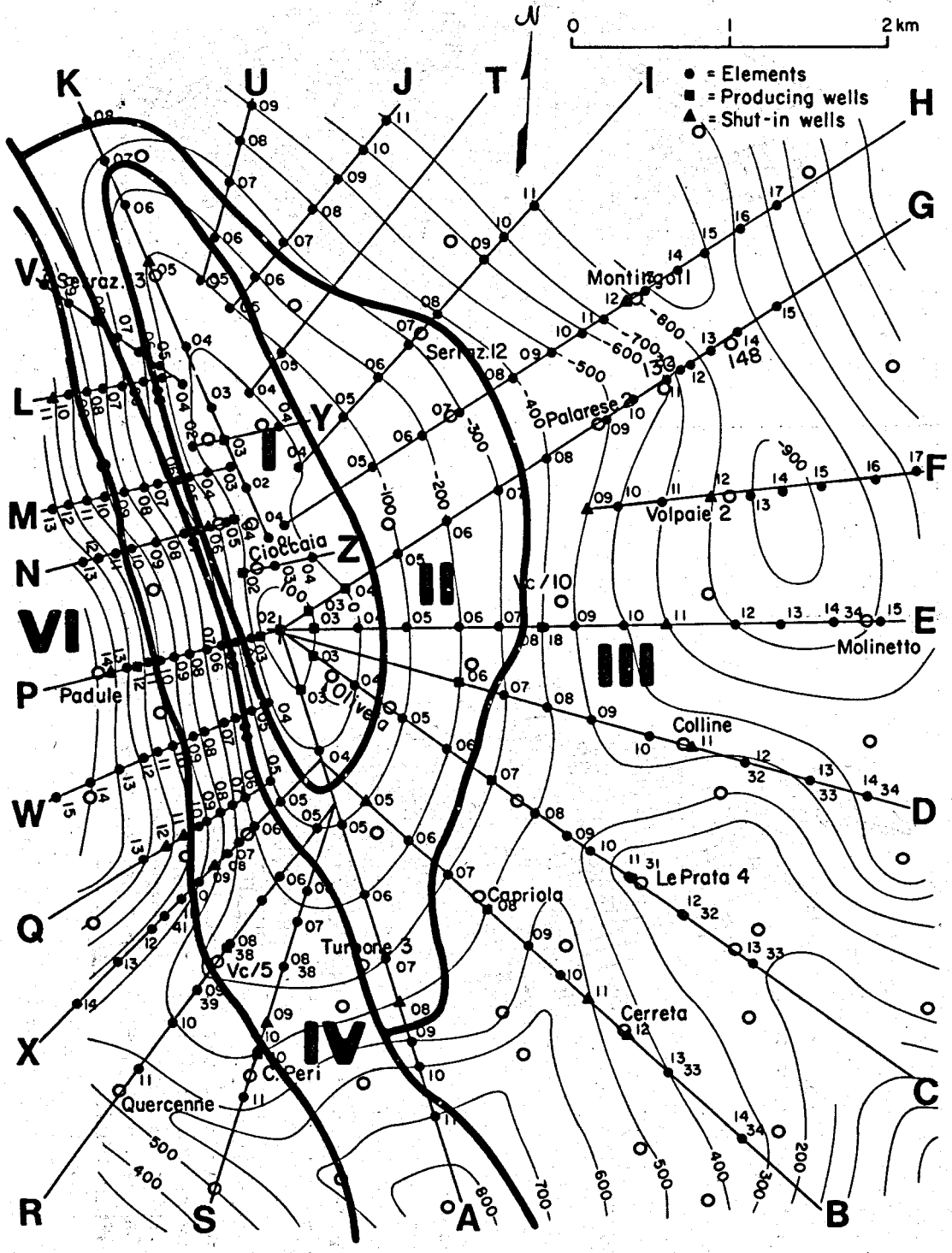

Fig. 1. Areal map of Serrazzano geothermal reservoir. (Thin lines—contours of caprock elevations; straight lines—geological cross sections; thick lines—boundaries of zones with different permeability) (XBL 797-7591B)

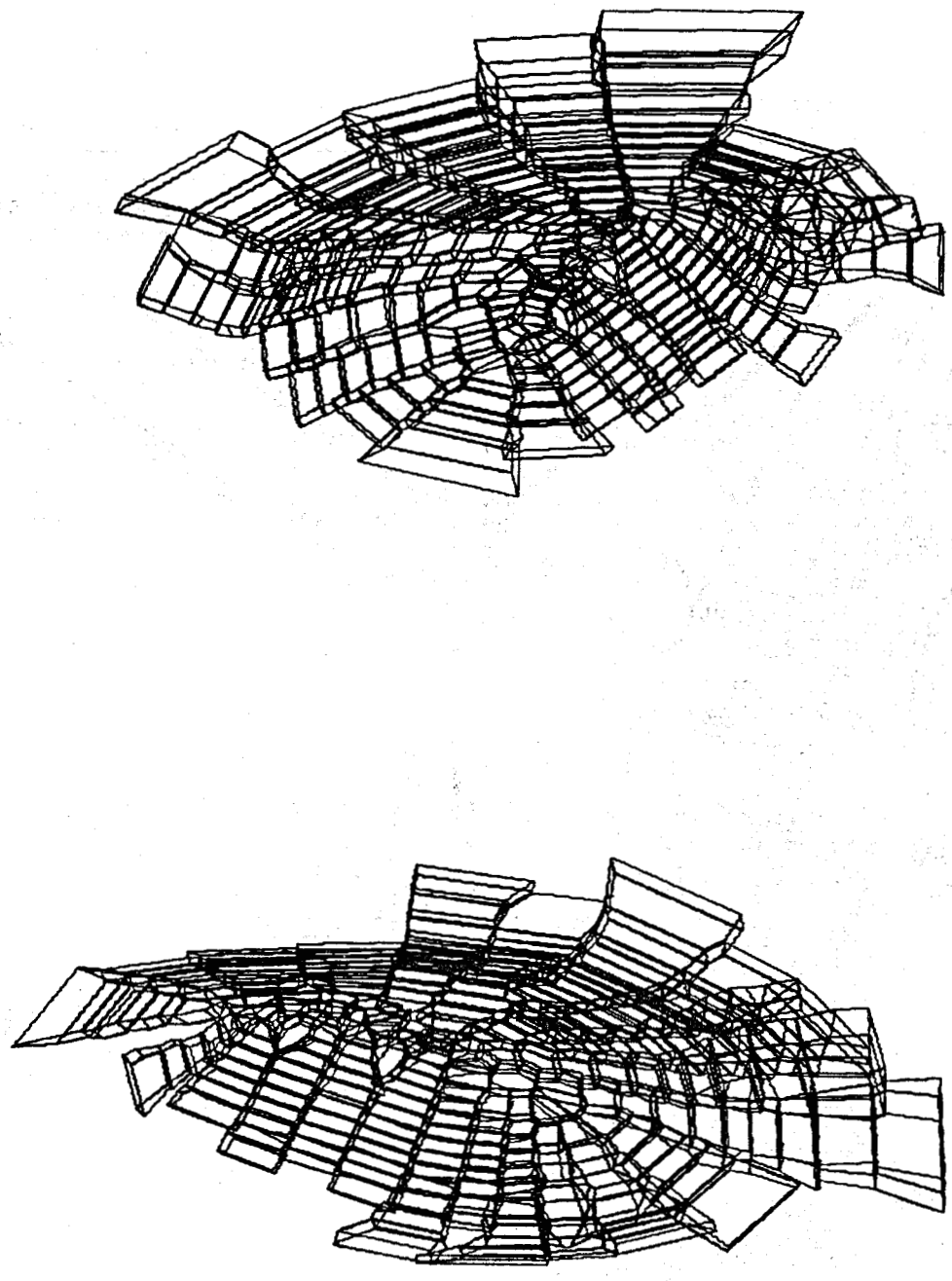

Fig. 2. Serrazzano mesh in rotated perspective views. (XBL 787-9570)

constant (well head) pressure. For modeling purposes, this could be imposed as a (mathematical) sink condition. The objective then would be to match observed production flow rates.

We chose a different approach, which makes a more sensitive use of the observed flow rate data. (These data are measured with good accuracy.) Namely, we impose observed flow rates on the simulated reservoir model. The task of the history match simulation then becomes one of (i) sustaining the observed flow rates over the period from 1959 to 1975, for which production data are available, and (ii) doing so under conditions of relatively mild pressure fluctuations near the main well field.

The history match simulation proceeds in trial-and-error fashion. We make certain assumptions for those parameters which are not well known, or are unknown, compare simulated field performance with observed performance, and then modify our parameter estimates so as to reduce discrepancies between simulated and observed performance. The limited availability of data (see Section 3) confronts us with a multitude of choices. It would appear that one could invoke a large variety of assumptions ad hoc, which may not be too meaningful, yet could not be refuted. The actual situation is, however, not anywhere near that ambiguous. The seemingly rather trivial requirement of sustaining observed flow rates at nearly constant pressures turns out to be very restrictive, due to the long duration of the simulation (15.5 years). The main well field near the structural high contains superheated steam, and therefore has a rather small mass content. The mass produced over 15.5 years is several hundred times larger than the mass in place in the main well field. Only through very subtle fine-tuning of certain parameters was it possible to avoid a premature catastrophic decline of pressures in the

main well field. Table 2 summarizes the handling of the various parameters during development of the history match.

Most important among the adjustable parameters is the permeability distribution. It determines the "dynamic" response of the reservoir; i.e., the way in which time-dependent production rates q(t) give rise to time-dependent pressures p(t). The permeability along the 1-phase flow path determines the short-term (days or weeks) "elasticity" of well field pressure response to fluctuations in production rates. Permeability distributions in the two-phase (boiling) region determine the extent to which pressure at the two-phase/steam interface can be maintained over periods of substantial depletion (years).

Under favorable circumstances, boiling rates away from the interface can be sufficiently large (equal to or larger than at the interface) to supply enough hotter steam to sustain temperature (hence pressure) at the interface. Then, the interface remains approximately stationary and at approximately constant pressure, while pressures decline away from the interface at the margins of the reservoir. The maps of average pressures as developed by Atkinson et al. (ref. 16) suggest that this type of behavior is present in Serrazzano.

A pattern of depletion with approximately stationary two-phase/steam interface at approximately constant pressure can prevail as long as the reserves of liquid water last. Reservoir performance during this period depends little on ultimate fluid reserves, and the simulation is not very sensitive to variations of those parameters which determine ultimate fluid reserves. These are mainly porosity ϕ and vapor saturation S in the two-phase zone. Therefore we have kept ϕ constant at a "best guess" of 10%.

Initial vapor saturation was chosen as follows. We compute relative

permeabilities from a version of Corey's equations:

$$k_{steam} = \begin{cases} (2r-S)\, S^3/r^4 & \text{for } S \leq r \\ 1 & \text{for } S \geq r \end{cases}$$

$$k_{liquid} = \begin{cases} (r-S)^4/r^4 & \text{for } S \leq r \\ 0 & \text{for } S \geq r \end{cases}$$

with the residual immobile water saturation taken as a somewhat arbitrary 1-r = 40%.

The pressure maps of Atkinson et al. show that pressure gradients at depth are less than 1/3 the hydrostatic gradient, from which we conclude that no mobile liquid water is present in the reservoir. Thus, initial liquid water saturation 1-S should not exceed 40%. We have taken S = 60% as initial

aquifers. We connected VC/10 to a large element representing a deep boiling aquifer, and adopted smoothly varying initial conditions throughout the mesh.

Apart from the inevitable adjustment in the case of VC/10, geometry and no-flow boundary conditions were kept fixed during the simulation. This was done chiefly because modifications based on simulation alone, without independent evidence, would seem rather arbitrary and speculative. Simulation results provide indirect evidence, however, that some cold water recharge is occurring near the margins, and that some steam reaches the main well field from outside the mesh (presumably through deep fractures.)

5. Results of History Match

Our current "best" model of the Serrazzano reservoir was arrived at, in its qualitative (conceptual) and quantitative features, through a large number of simulations. Parameters had to be adjusted again and again to rectify deficits in the simulated reservoir performance. It turned out to be very difficult to sustain observed flow rates throughout the entire modeling period (1959-1975), without "overshooting" pressures in the main well field for the first few years. This difficulty gives important clues to what is happening in the field (see below).

Our model cannot resolve all of the uncertainties about parameters characterizing Serrazzano field. It remains in part speculative, and needs to be further checked and refined as more data become available. We do believe, however, that the model is plausible in view of general ideas about Serrazzano. And it appears reasonable in that it accounts for important trends and features observed in the field.

Qualitatively, the reservoir model is that of a steam cap overlying a boiling aquifer. There is dry steam in the center, near the structural high

(where the main well field is located). Pore water (i.e., two-phase zones) is confined to the margins. Water is immobile throughout. It boils in place as steam flows to the wells. The two-phase/steam interface, located at approximately -500 m (see Figure 1) acts as a nearly constant pressure boundary for the dry steam region. Gravity effects are small as only steam is mobile.

In order to sustain field production over the entire 15.5-year period modeled, we had to introduce 6 zones of different permeability (see Figure 1 and Table 3). Zone I includes the main well field. Its very high permeability is necessitated by the observation that production rates at individual wells can fluctuate appreciably without very strong pressure response. Zones II and IV are essentially regions of dry steam flow, with permeabilities adjusted such as to provide proper resistance to steam flowing from the two-phase margins toward the main well field at the center of the reservoir. Zones III and VI are essentially two-phase regions, with permeabilities such as to obtain a pattern of nearly uniform boiling and hence good pressure maintenance at the two-phase/steam interface during depletion. Zone V is the deep boiling aquifer. The time-dependence of simulated average steam pressures is shown in Figure 3. Values for the slope of pressure decline versus cumulative production (dp/dQ) deduced from this figure are given in Table 4 for the entire simulated period as well as for the post-1967 period. Average simulated pressure decline in the reservoir is somewhat slower than the value $dp/dQ = -1.9 \times 10^{-10}$ bar/kg as deduced from field data by Atkinson et al.[16]

Table 5 gives mass balances for the various zones, as well as for the entire reservoir. It is seen that Zones III and VI contribute roughly equal amounts to cumulative field production. Over 15 years the field loses 18.2% of the mass present on 1/1/60. Total mass reserves are approximately

ZONE	PERMEABILITY (milliDarcy)
I	4000
II	90
III	85
IV	25
V	85
VI	40

Table 3 : Permeability Distribution. The zones are defined in Figure 1.

REGION	-dp/dQ (10^{-10} bar/kg) 1960-75	1967-75
III	.74	1.10
VI	1.91	2.29
entire reservoir	.75	1.35

Table 4 : Simulated Pressure Decline

REGION	Vapor Saturation (%) 1960	1975	Mass Content (10^8kg) 1960	1975	Mass Loss 10^8kg	%
I	100	100	1.89	1.84	.05	2.6
II	99.9	100	6.37	4.97	1.40	22.0
III	69.0	73.8	1108.8	950.3	158.5	14.3
IV	83.9	86.5	87.2	74.3	12.9	14.8
VI	60.7	72.6	464.3	333.3	131.0	28.2
R	73.3	78.5	1668.7	1364.8	303.9	18.2

Table 5 : Simulated Mass Balances

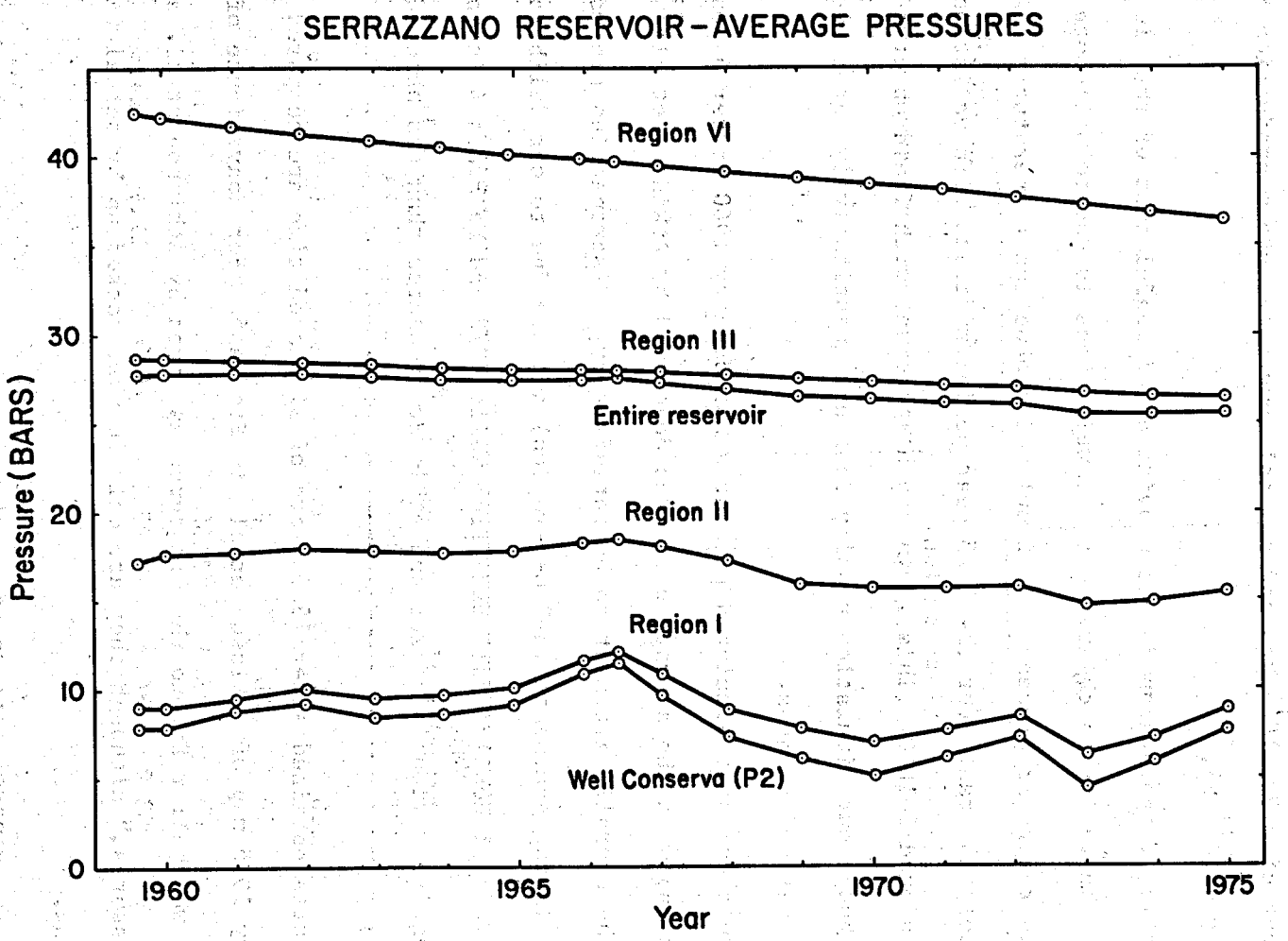

Fig. 3. Simulated average pressures. (XBL 807-1402)

1.7×10^{11} kg in 1960, and 1.4×10^{11} kg in 1975. These values are entirely consistent with Weres' estimate of an initial (pre-exploitation) mass content of 2.3×10^{11} kg, and a total cumulative steam production to date of 0.9×10^{11} kg.[18]

Production temperatures do not provide a meaningful test of the simulation, as much of the variation observed at the well heads is due to well-bore effects rather than reservoir processes.[8] Simulated production temperatures are approximately constant over the 15.5 year period modeled, with variations typically around 5-10°C. This is in rough agreement with field observations, although our simulation usually does not quantitatively agree with the small observed changes.

Figure 4 compares simulated pressures for January 1960 (after 6 months of simulation) with the average pressures developed by Atkinson et al.[16] We consider the overall agreement to be satisfactory. Discrepancies are most pronounced in the southeast (A-B-C-D-region) and are due to our deliberate choice of initial conditions: data from wells VC/2 and Le Prata 4 indicate that the entire region is cooler and at lower pressures than was assumed in reference 16.

Pressures obtained after 15.5 years of simulated time are compared with the January 1975 map of Atkinson et al. in Figure 5. For convenience of discussion we shall refer to the pressures as given by Atkinson et al. as "field pressures," although they are only in part backed up by actual field observations.

While the general pattern of simulated pressures does resemble the "field pressures," for the most part there is no quantitative agreement in detail. Overall, simulated pressures are somewhat high. This is particularly

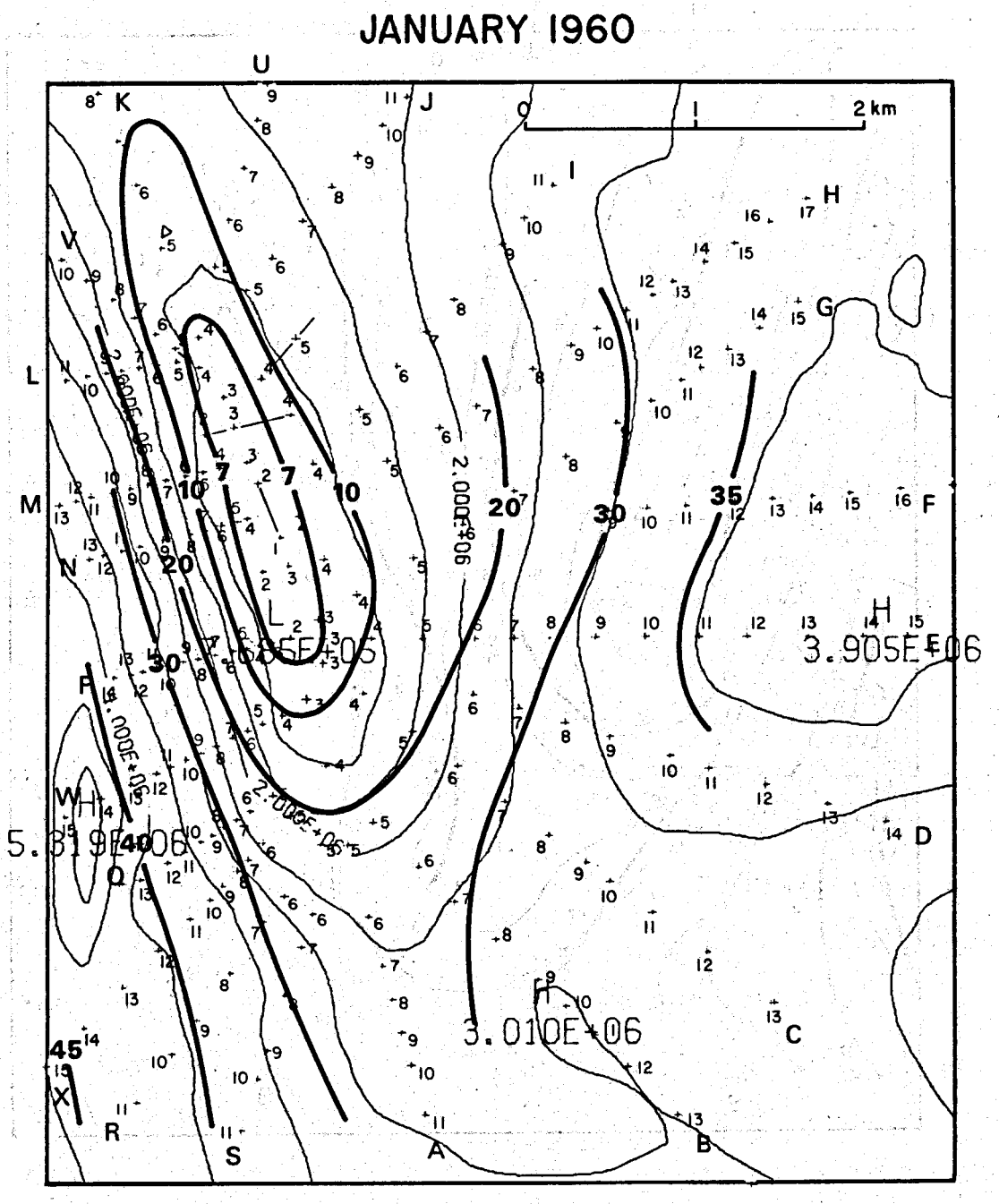

Fig. 4. Pressure distribution for January 1960. The thick contours are based on field observations (units: bars), whereas the thin contours are simulated results (units: Pascals). The simulated results refer to the lowest layer of the reservoir model. Simulated vertical pressure variations are small (≈1 bar). Pressure increments between contour lines are 5×10^5 Pascal ≡ 5 bar. (XBL 807-1401A)

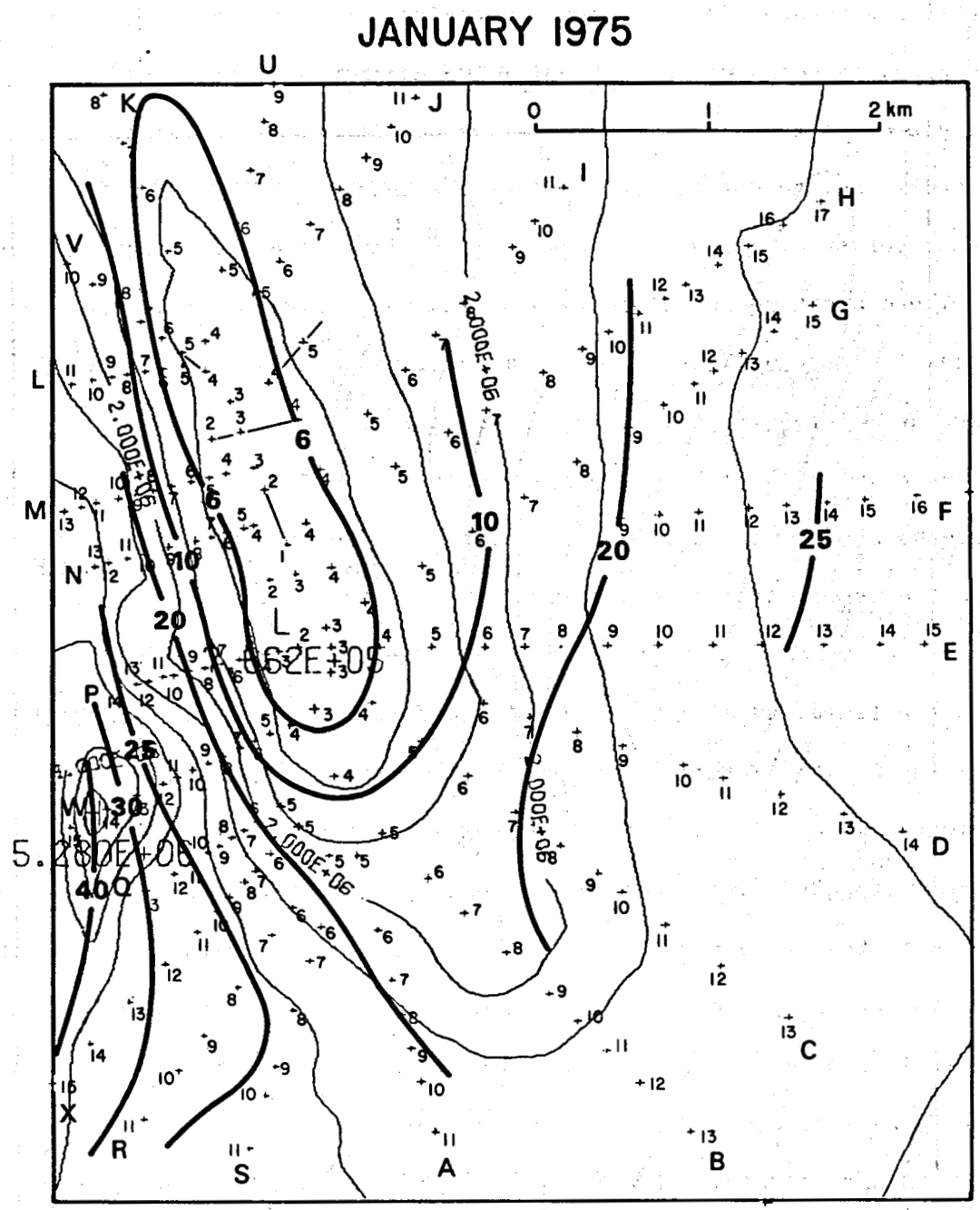

Fig. 5. Pressure distribution for January 1975. (XBL 807-1401B)

evident for pressures in the two-phase region, roughly corresponding to $p > 20$ bars, in both the eastern and western margins of the field. In our model, pressures in the two-phase regions decline solely as a consequence of temperature decline due to heat loss of the rock in boiling water. As we do impose proper steam production rates, we should obtain correct overall heat loss. There are three possible reasons why for a given overall heat loss pressures in the two-phase region could decline more rapidly in the field than in our model: (i) intrusion of some colder water into depleting two-phase zones would lower temperatures, hence pressures; (ii) the volume of the two-phase zone may be somewhat smaller than assumed in our model, either because the reservoir may be somewhat thinner, or because the two-phase/steam interface may be at a depth greater than 500 m ; (iii) heat transfer from the rock to the fluid may be inhibited because some of the permeability may be due to isolated fractures rather than the rock matrix. These effects are further investigated in Chapter 6. Pressures are also somewhat high near the main well field (N4-A3-G4-area). This is probably not entirely due to too high pressures in the two-phase region. The 20 bar contour, which roughly coincides with the two-phase/steam interface, agrees fairly well with the field pressures in the west, without overshooting excessively in the east. Thus, in order to make simulated pressures smaller near the main well field, we would need to diminish permeability along the l-phase flow path. This, however, would make it impossible to sustain the higher flow rates of the early 1960's. We believe that this difficulty may indicate that some of the steam supply to the main well field originates from deep fractures, rather than from that portion of the reservoir which is simulated in our present model.

Additional support for this hypothesis is provided by the peculiar depletion pattern observed during the simulation. Although simulated pressure decline in the reservoir margins is somewhat slower than observed in the field, we found it quite difficult to sustain the observed flow rates in the main well field. This could only be achieved by fine-tuning the permeability distribution carefully in the two-phase regions such as to optimize pressure maintenance at the two-phase/steam interface. This was achieved by making permeabilities in the two-phase regions rather "large," so that boiling would easily spread all the way to the hotter margins rather than being concentrated near the two-phase/steam interface. Resulting boiling rates are almost uniform throughout, and are actually increasing somewhat away from the interface toward the margins. During the entire simulation period, vapor saturations increase almost uniformly throughout the two-phase region, and the two-phase/steam interface remains stationary. These simulated results support some of the choices made with regard to initial distribution of pore water in 1959, namely, to place the two-phase/steam interface near 500 m depth, where it is believed to have been in the pre-exploitation state, and to take initial vapor saturation to be constant ($S = 60\%$) throughout the two-phase zone. Thus, the model evolves in a way which is consistent with our assumptions for initial distribution of pore water. The extent to which we had to fine-tune the permeability distribution to achieve uniform boiling (and actually going somewhat beyond) in order to sustain production may indicate that in actuality not all production is generated through boiling in the two-phase zone modeled. The results seem to suggest that an as yet undetermined amount of steam enters the main well field through fractures from depth, perhaps at a rate of a few kg/sec.

6. Additional Temperature Decline

We noted before that simulated average pressure decline is slower than observed in the field. In order to obtain a pressure decline of $dp/dQ = -1.9 \times 10^{-10}$ bar/kg, as suggested in ref. 16, an additional average pressure drop of $\delta p \approx 3.5$ bar is required in the two-phase regions. At an average initial temperature $T \approx 240\ ^{o}C$ this corresponds to an additional temperature decline of $\delta T \approx 5\text{-}6\ ^{o}C$. We shall now examine the effects mentioned in Chapter 5 to see which could be likely candidates for producing such a temperature decline.

6.1 Intrusion of Cold Water

In order to assess this effect we compute mixing temperatures for cold water and a hot rock/water/steam reservoir. We start with a reservoir temperature of $T = 240\ ^{o}C$ and a vapor saturation of $S = 67.5\%$, corresponding to the average vapor saturation in the two-phase region obtained after 15.5 years of simulation for the Serrazzano model. Results for additional temperature decline δT as a function of cold water recharge are plotted in Figure 6 for the cases of recharge water temperature $T_w = 20\ ^{o}C$ and $T_w = 80\ ^{o}C$. If recharge is equal to discharge, the system ends up at a vapor saturation $S = 60\%$, equal to the initial value, with an additional temperature decline $\delta T = 2\ ^{o}C$. Recharge would have to exceed twice the discharge in order to yield a δT of $5\ ^{o}C$.

These estimates and the curves in Figure 6 are based on a model of "uniform mixing," i.e., with the recharge waters being uniformly distributed throughout the boiling volume. This model may not be very realistic, because

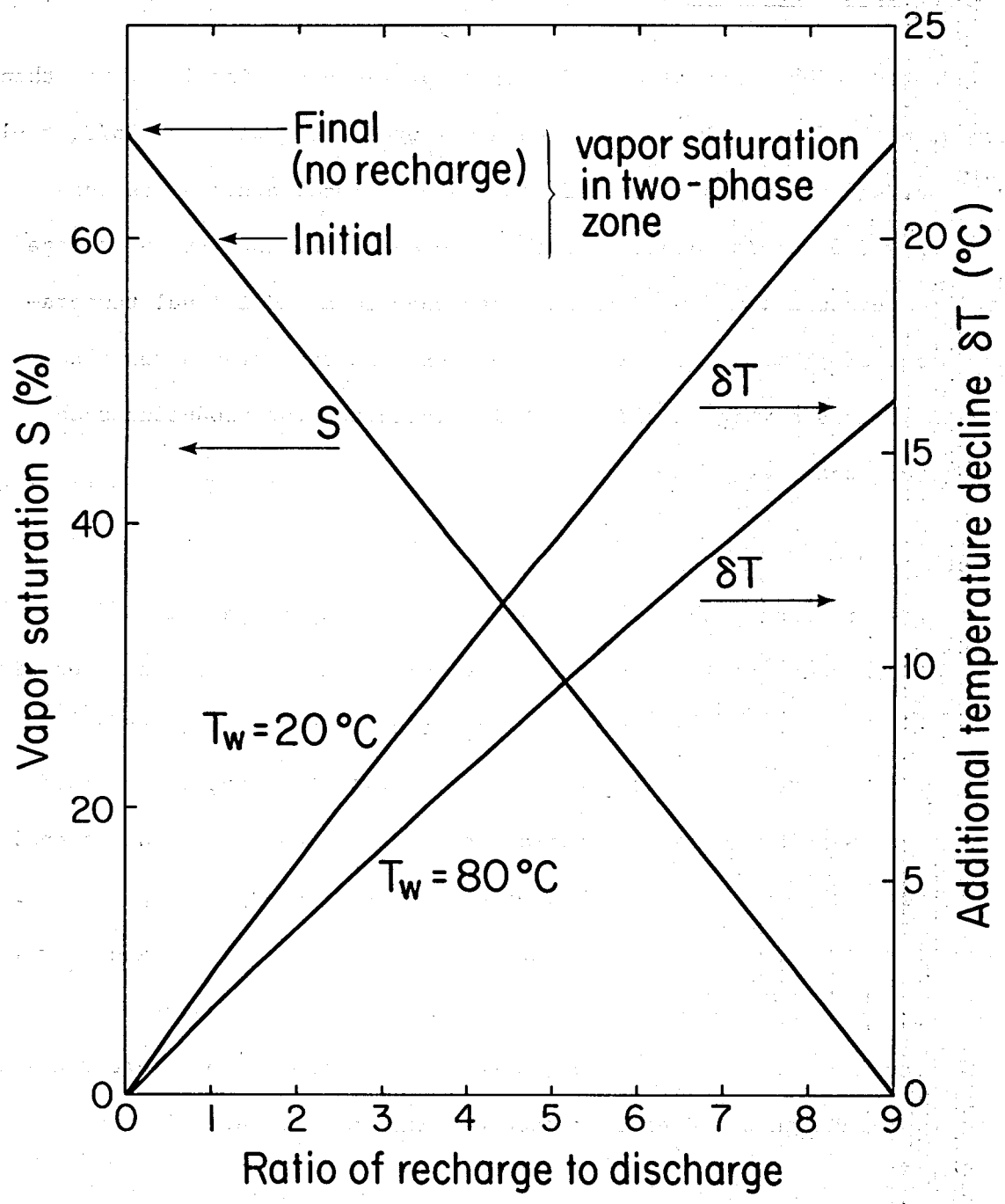

Figure 6. Effects of Cold Water Intrusion. (XBL 808-2725)

recharge waters may instead move from the reservoir margins inward as rather sharp fronts. In the latter case the water flowing into the boiling zone would have been heated up to original reservoir temperature, so that our model, above, would overestimate temperature decline. This suggests that, while recharge could make a significant contribution, it is in all likelihood not a major source of the additional temperature decline.

6.2 Lower Two-Phase/Steam Interface

The total amount of steam produced from the two-phase region in 15.5 years (1959-75) is $Q = 2.94 \times 10^{10}$ kg. Virtually all of this is generated through boiling, in which the rock transfers a total amount of 5.36×10^{16} J of heat to the fluid (corresponding to an average vaporization enthalpy of $h_{vap} = 1.82 \times 10^{6}$ J/kg). If the 1959 initial conditions were modified such as to extend the region of large vapor saturation to greater depth, boiling would be confined to a smaller volume. In order to supply the same amount of heat for vaporization, the rock temperature would have to decline by a larger amount.

In Figure 7 we have plotted the reservoir volume V_D below depth D as a function of depth. The two-phase zone has a volume of 4.94×10^{9} m^3, corresponding to an average depth of the two-phase/steam interface of -479 m. Figure 7 also shows the additional temperature decline δT that would result from a lowering of the two-phase/steam interface. In order to yield a δT of 5-6 ^{o}C, the interface would have to be lowered to a depth of -680 to -700 m. Such a value, while somewhat large, is not incompatible with Weres' model of hydraulic continuity between the pre-exploitation reservoir and surrounding aquifers. With a typical elevation of +100 m for the water table, the vapor pressure at the two-phase/steam interface would have to balance a column of

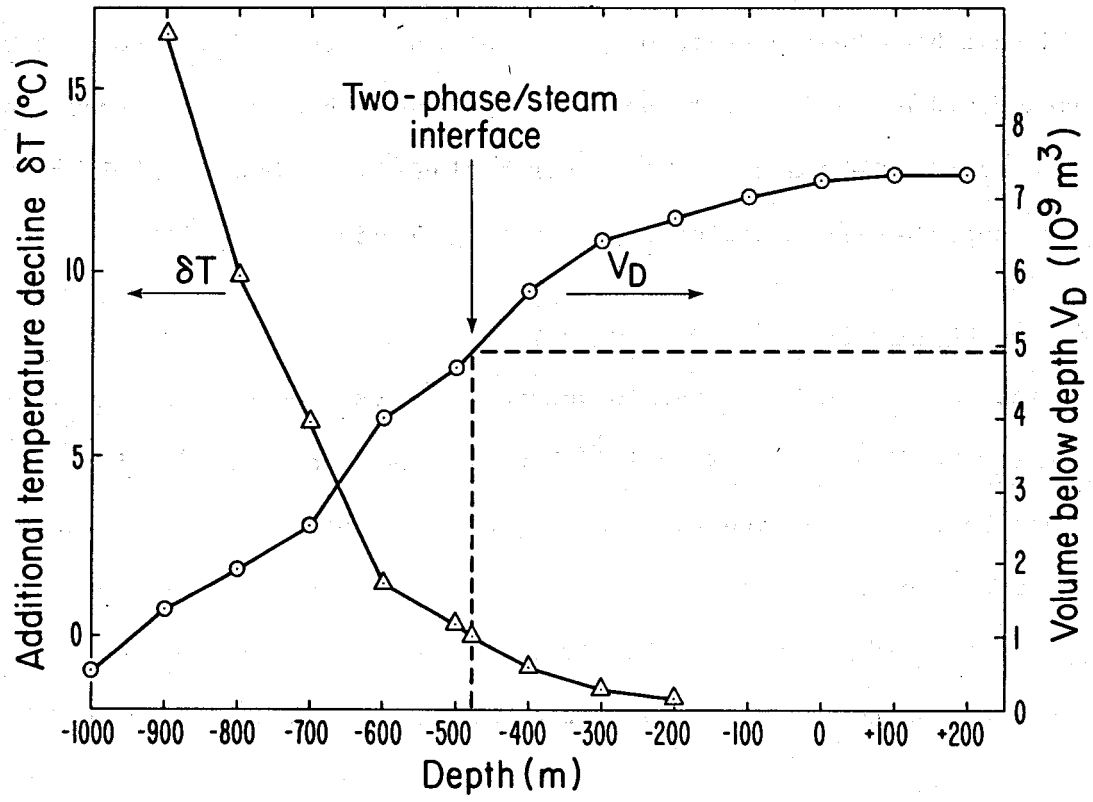

Figure 7. Temperature Decline in Dependence of Assumed Depth of Two-Phase/ Steam Interface. (XBL 808-2727)

800 m water. Assuming a linear dependence of water temperature and density upon depth, the required pressure is 69 bars, corresponding to a pre-exploitation temperature at the two-phase/steam interface of 285 °C. A closely related possibilitiy is that the top of the two-phase zone may have a rather small liquid saturation in 1959, and dry up during subsequent production.

It is to be noted that the effect discussed above comes about from a reduction of the volume of the boiling zone. An alternative to reducing the volume by lowering the two-phase/steam interface would be to decrease the thickness of the reservoir by an appropriate amount (about 50% for a $\delta T \approx 6$ °C, see Figure 7). The data available to us do not allow to distinguish between these alternatives.

6.3. Incomplete Thermal Equilibration between Rock and Fluid

Fractures are known to play an important role in fluid transport in Serrazzano. It appears possible that parts of the reservoir have low matrix permeability. As steam is produced, the water in the more permeable regions boils, extracting heat from the rock matrix and lowering its temperature. Subsequently heat will flow mainly by conduction from the less permeable rock into the flow regions. The temperature decline in the boiling region will be more rapid, and in the impermeable rock less rapid, than would be observed if water and rock were mixed throughout the entire volume. The additional temperature decline δT occurring in the flow region because of incomplete temperature equilibration between flow- and no-flow-regions will increase with (i) boiling rate, (ii) fraction of impermeable rock volume, and (iii) size of the embedded low-permeability reservoir regions.

We have applied SHAFT79 to make a parametric study of these effects. The model reservoir consists of a large number of identical "elementary units" (see Figure 8). The elementary unit is a cube, the outer part of which consists of porous (or highly fractured) and permeable material, whereas the inner part is a (centered) cube of solid impermeable rock (see Figure 9). As we are interested in a process of slow and very nearly uniform depletion, flow between elementary units is negligible and only one elementary unit needs to be modeled. Initial conditions were chosen as $T = 240\ ^{o}C$, $S = 60\%$, representative of initial conditions (1959) in the two-phase zone of the Serrazzano reservoir. At the surface of the elementary unit a constant production rate of 1.75×10^{-8} kg/m^{3}s is applied. This gives rise to a boiling rate of very nearly the same magnitude, which corresponds to what is observed in the Serrazzano simulation. Calculations were done for impermeable rock volumes of 90%, 80%, and 50%, respectively, of the elementary unit volume. Average porosity is held fixed at 10%, so that the porosity in the flow region is 100%, 50%, and 20%, respectively, in the three cases.

Figure 10 shows the dependence of additional temperature decline upon length L of the elementary unit. The side length of the impermeable rock cube is $L \times .9^{1/3}$, $L \times .8^{1/3}$, and $L \times .5^{1/3}$ for the cases of 90%, 80%, and 50% impermeable rock volume, respectively. The case with 90% impermeable volume, corresponding to 100% porosity in the flow region, provides an upper bound for temperature decline. The cases with 80% and 50%, respectively, are more plausible and potentially realistic. A length $L \approx 200$ m produces temperature declines of the magnitude needed to make simulated reservoir performance agree on average with observed performance. 200 m is to be considered a characteristic length of our model. In actuality, of course,

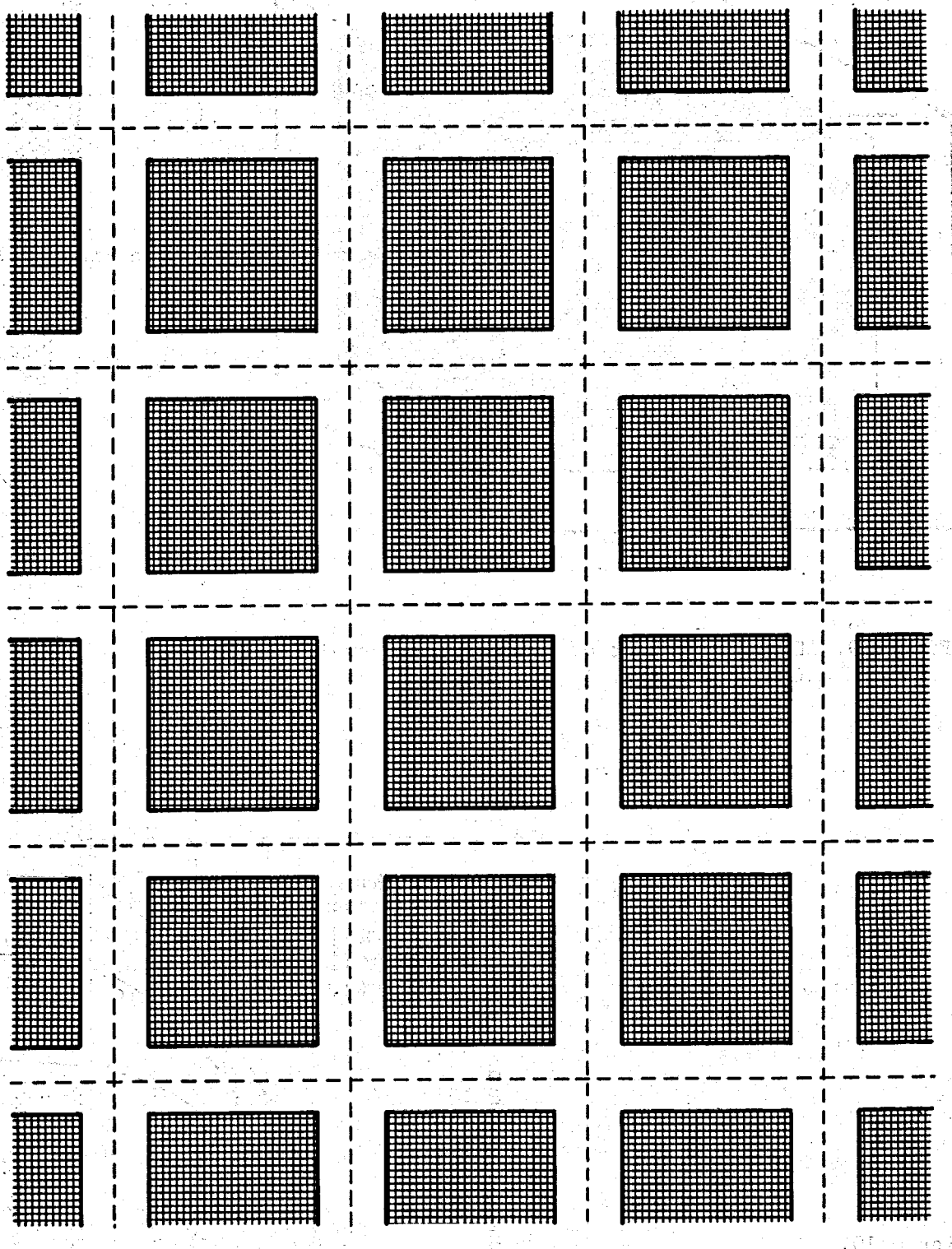

Figure 8. Areal View of Fractured Reservoir Model. (XBL 808-2723)

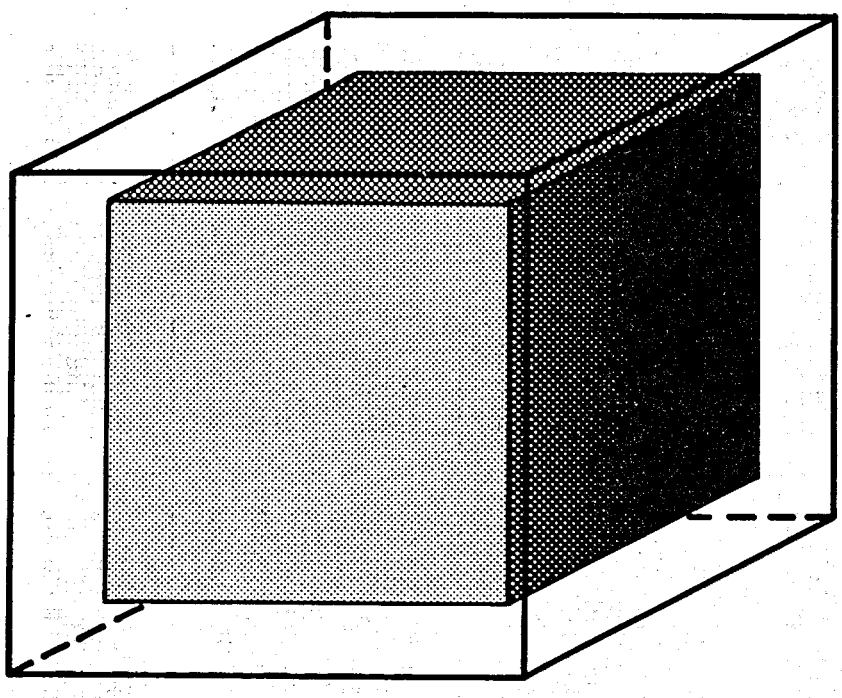

Figure 9. Elementary Unit of Fractured Reservoir. (XBL 808-2724).

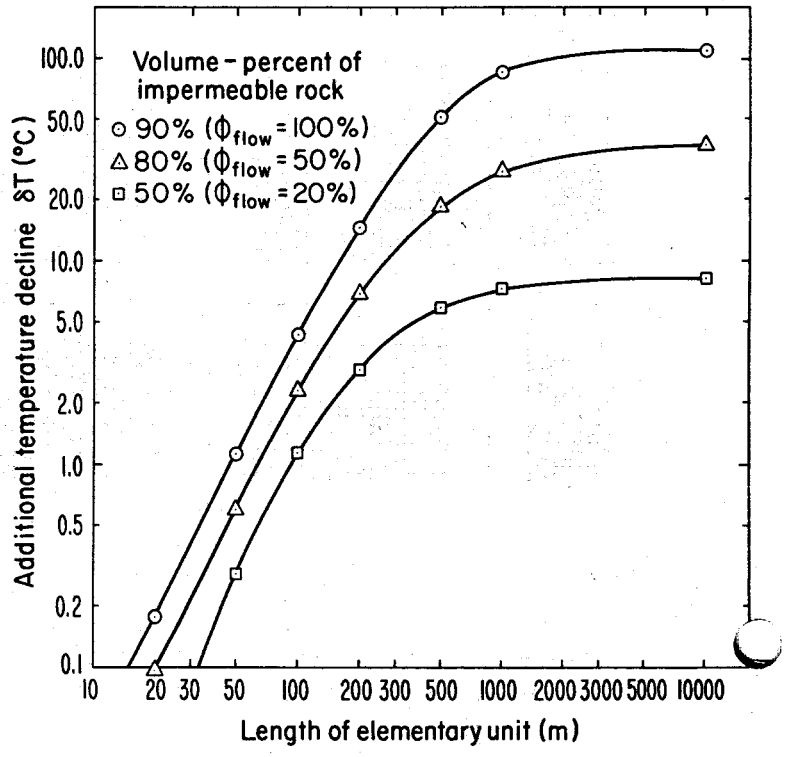

Figure 10.

Effects of Incomplete Thermal Equilibration between Rock and Fluid. (XBL 808-2726)

the reservoir rock need not be regular, and sizes of impermeable regions could vary throughout the reservoir. It appears entirely possible, particularly in view of the large number of unproductive wells, that such large impermeable rock masses could be present interspersed with permeable regions in the reservoir. We suggest, therefore, that incomplete temperature equilibration could well be a major source of additional temperature decline in the field.

In conclusion, both a diminished volume of the two-phase zone or incomplete thermal equilibration between vapor and fluid could very significantly increase the rate of temperature and pressure decline. These two effects could separately or combined account for an additional temperature decline of 5-6 ^{o}C over the simulated period of 15.5 years, such as is required to make simulated average pressure decline agree with the value deduced from field data.

7. Reservoir Performance 1975-1990

The history match from 1959 to 1975 provides a model of Serrazzano reservoir which can be used to extrapolate (forecast) production at a later time. For this, we assume constant well head pressure p = 5 bars. Discharge is simulated by connecting all well elements to a very large element with constant pressure p = 5 bars. Interface areas are adjusted such that proper (measured) production rates are obtained for January 1975, which is the most recent time for which digitized production data were available. The simulation has been extended through January 1990, with results given in Figures 11 through 16 and Table 6.

Total simulated mass production from 1975 to 1990 is 29.8 x 10^9 kg, corresponding to an average rate of 63.0 kg/sec. Average produced enthalpy is

well	location	PRODUCTION RATE (kg/sec) January 1975	January 1990	decline (%)
BCF/3	WCA3	2.90	2.30	20.9
Capriola	WCB8	12.95	10.76	17.0
Oliveta	WCC3	1.41	1.13	19.7
VC/2	WCC7	0.81	0.66	18.6
Le Prata 4	WEC31	5.35	4.62	13.7
Grottitana	WCD6	3.89	2.87	26.0
Soffionissimo 1	WCE3	2.61	2.11	19.3
Le Vasche	WCG3	3.32	2.67	19.7
Vignacce	WCG4	6.18	5.00	19.2
Pozzaie 2	WEN4	5.46	4.47	18.2
Conserva	WCP2	3.51	2.81	20.0
Avalle 2	WCP3	4.44	3.55	20.0
Lustignano	WCP12	9.89	5.69	42.5
VC/5	WER38	2.33	1.70	27.1
Campo ai Peri	WES40	2.42	1.82	24.6
#8	WCY3	1.33	1.09	18.4
Cioccaia	WCZ2	2.99	2.42	19.3
aggregate*		71.8	55.7	22.4

Table 6: Well-by-Well Production Rates for 1975 and 1990.

* does not include well VC/10.

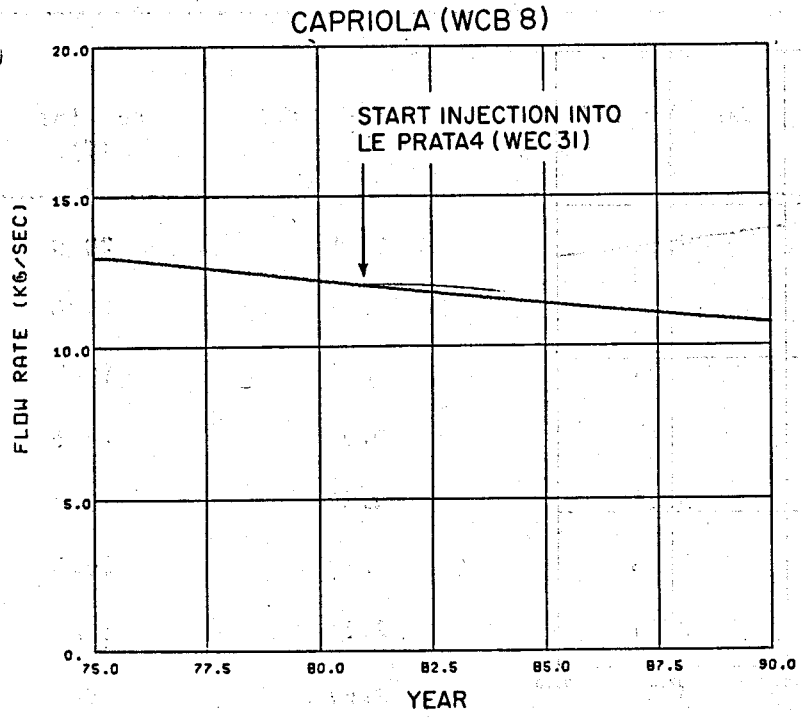

Figure 11. Production Forecast for Well Capriola (WCB8) with and without Injection. (XBL 809-2810)

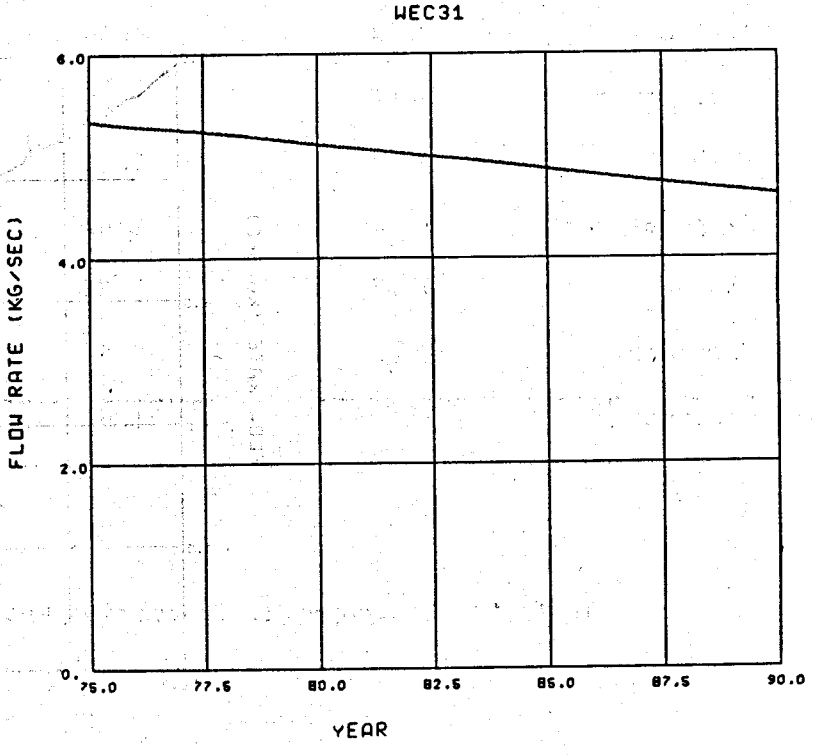

Figure 12. Production Forecast for Well Le Prata 4 (WEC31). (XBL 809-11950).

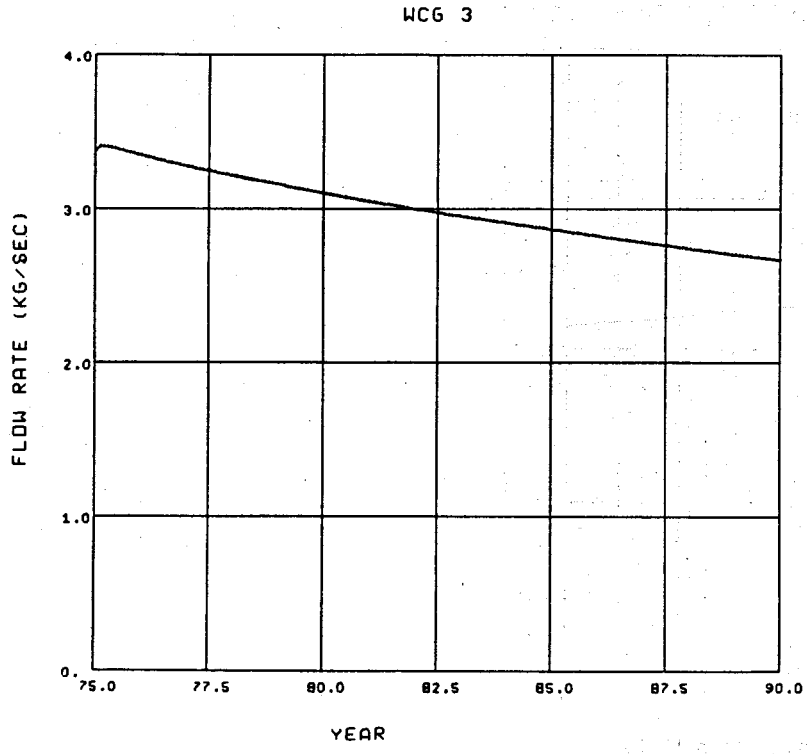

Figure 13. Production Forecast for Well Le Vasche (WCG3). (XBL 809-11949)

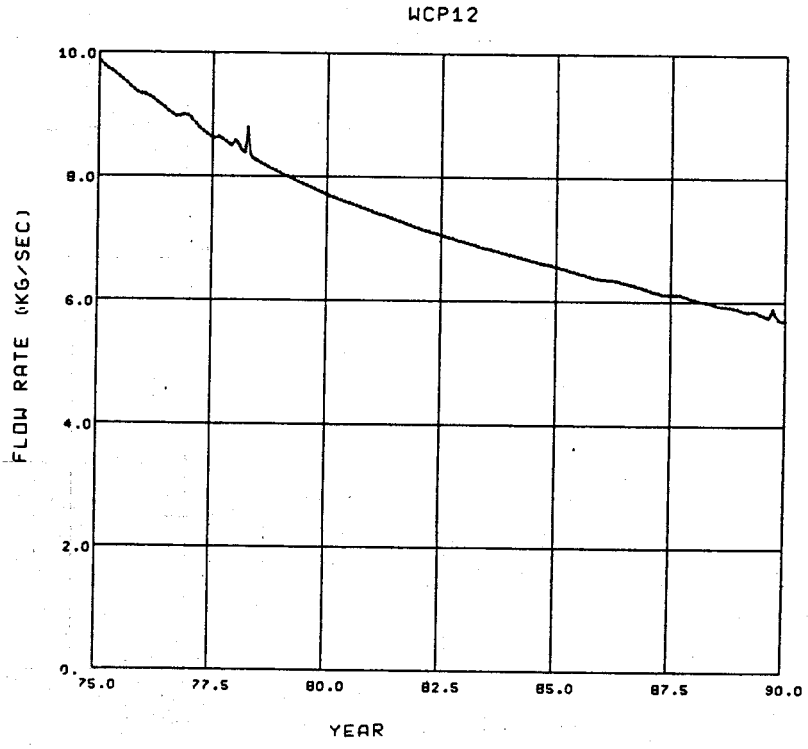

Figure 14. Production Forecast for Well Lustignano (WCP12). (XBL 809-11948)

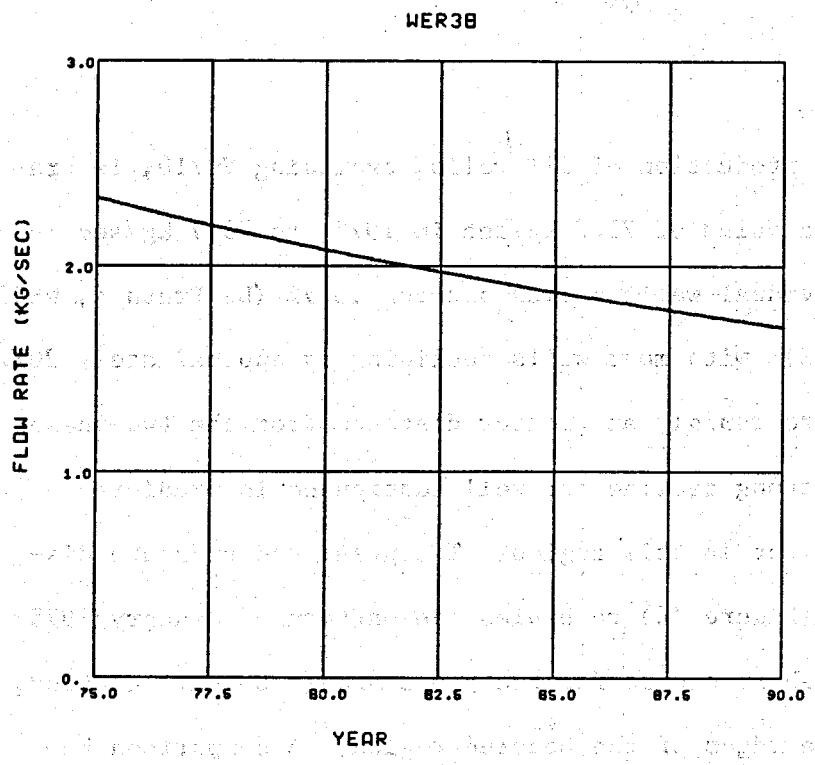

Figure 15. Production Forecast for Well VC/5 (WER38). (XBL 809-11951)

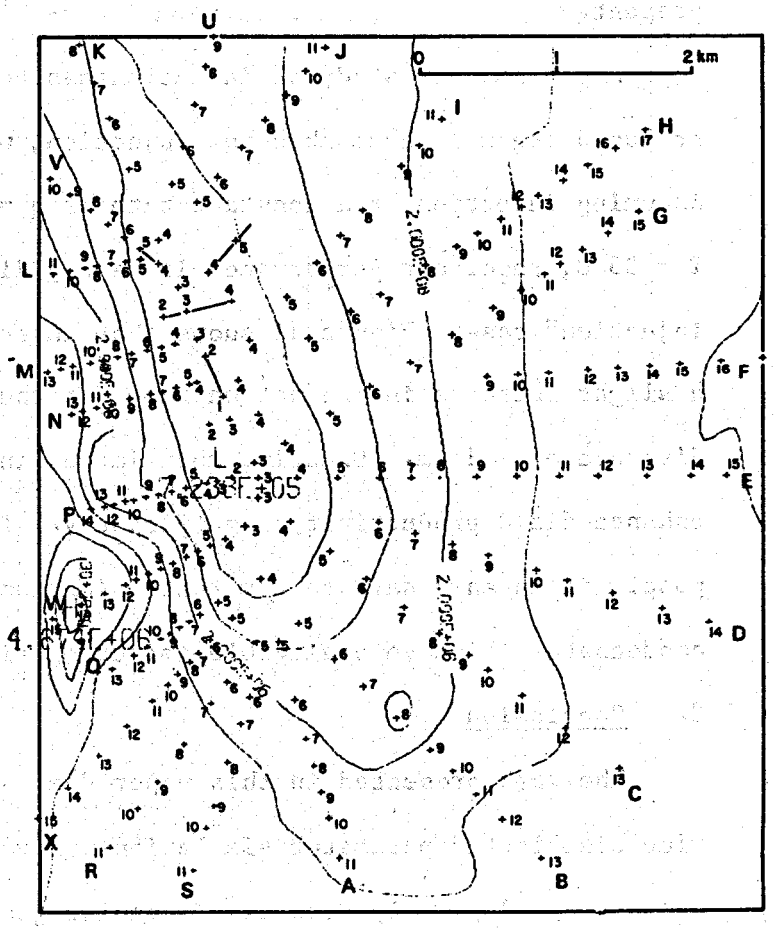

Figure 16. Predicted Reservoir Pressures for January 1990. (XBL 809-2809)

2.851 MJ/kg. The aggregate production of all wells, excluding VC/10, is predicted to drop by 24% from a value of 71.8 kg/sec in 1975, to 55.7 kg/sec in 1990. The decline for individual wells varies between 13.7% (Le Prata 4, WEC31) and 42.5% (Lustignano, WCP12), with most wells declining by approximately 20%. Generally, wells decline more rapidly at greater distance from the two-phase zones. The exceptionally strong decline for well Lustignano is predicted because the reservoir dries out in this region. The predicted pressure distribution for January 1990 (Figure 16) resembles the pattern of January 1975 (Figure 5). The strongest shift occurs for the p = 3 MPa (= 30 bar) contour, which has been pushed to the edges of the modeled region. A comparison between predicted and observed flow rates is planned for the period from 1975 - present.

A preliminary study of injection has been made. Approximately 20% of the produced steam is available for injection, which is a rather small amount. Assuming injection at a constant rate of q = 13 kg/sec, at a temperature of $T = 35^{\circ}C$, reservoir performance is hardly distinguishable from the "no injection" case. Figure 11 shows that injection into Le Prata 4 (WEC31) causes a slight increase in production rate for the nearest well Capriola (WCB8) at a distance of $\approx$ 1 km. Clearly, much larger injection rates would be required to enhance field productivity significantly. From the point of view of fluid disposal, it appears safe to say that injection of the small amount of available condensate will have negligible impact on field performance.

8. Conclusion

The work presented in this paper demonstrates the feasibility of field-wide distributed parameter simulations of vapor-dominated geothermal reservoirs in geologically accurate irregular geometry. The simulated model is

self-consistent and shows semi-quantitative agreement with field data. We believe that the simulation provides evidence for the validity of the physical model and mathematical methods used in the simulator SHAFT79.

The simulated field behavior substantiates a conceptual model of Serrazzano reservoir as a steam cap overlying a boiling aquifer. Comparison with actual field behavior suggests a smaller volume of the boiling zone than was previously assumed and/or incomplete heat transfer due to fractures at the margins, and significant upflow of steam from depth through fractures.

Application of numerical simulation for well-by-well production forecasting has been demonstrated. A brief study of injection of available condensate indicates negligible impact on field performance.

Acknowledgments

This work was supported by the U.S. Department of Energy under Contract No. W-7405-ENG-48. Thanks are due to N.E. Goldstein and M. J. O'Sullivan for a critical reading of the manuscript.

Nomenclature

C_R	specific heat of rock, J/^oC kg
H	thickness of reservoir, m
K_R	thermal conductivity of rock, W/m^oC
k	absolute permeability, milliDarcy ($\approx 10^{-15} m^2$)
k_{liquid}	relative permeability of liquid, fraction
k_{steam}	relative permeability of steam, fraction
L	length of elementary reservoir units, m
p	pressure, Pascal or bar ($\equiv 10^5$ Pascal)
Q	fluid production, kg
q	rate of fluid production, kg/s
r	parameter for relative permeability functions, dimensionless
S	volumetric vapor saturation, fraction
T	temperature, ^oC
t	time, s
ρ_R	rock density, kg/m^3
ϕ	porosity, dimensionless

References

1. Pruess, K., and Schroeder, R.C.: "SHAFT79 User's Manual," Lawrence Berkeley Laboratory Report LBL-10861 (March 1980).

2. Pruess, K., and Schroeder, R.C.: "Geothermal Reservoir Simulation with SHAFT79," Proc., Fifth Stanford Workshop on Geothermal Reservoir Engineering, Stanford, Ca. (1980), 183-188.

3. Pruess, K., Bodvarsson, G., Schroeder, R.C., Witherspoon, P.A., Marconcini, R., Neri, G., and Ruffilli, C.: "Simulation of the Depletion of Two-Phase Geothermal Reservoirs," paper SPE-8266, presented at the 54th Annual Fall Technical Conference and Exhibition of the SPE of AIME, Las Vegas, Nevada, 1979.

4. International Formulation Committee: "The 1967 IFC Formulation for Industrial Use, A Formulation of the Thermodynamic Properties of Ordinary Water Substance," (February 1967).

5. Duff, I.S.: "MA28 - A Set of Fortran Subroutines for Sparse Unsymmetric Linear Equations," Report AERE-R 8730, Harwell, Oxfordshire, Great Britain (June 1977).

6. O'Sullivan, M.J.: "A Similarity Method for Geothermal Well Test Analysis," Lawrence Berkeley Laboratory Report LBL-10968 (March 1980); submitted to Water Resources Research.

7. O'Sullivan, M.J., and Pruess, K.: "Analysis of Injection Testing of Geothermal Reservoirs," Lawrence Berkeley Laboratory Report LBL-10985 (June 1980); to be presented at the 1980 Annual Meeting, Geothermal Resources Council.

8. Nathenson, M.: "Some Reservoir Engineering Calculations for the Vapor-Dominated System at Larderello, Italy," USGS open file report 75-142, Menlo Park, Ca. (1975).

9. Cataldi, R., Stefani, G., and Tongiorgi, M.: "Geology of Larderello Region (Tuscany): Contribution to the Study of the Geothermal Basins," in: Tongiorgi, E. (ed.), Nuclear Geology on Geothermal Areas, Spoleto (1963), 235-267.

10. Marconcini, R., McEdwards, D., Neri, G., Ruffilli, C., Schroeder, R., Weres, O., and Witherspoon, P.: "Modeling Vapor Dominated Geothermal Reservoirs," Proc., Larderello Workshop on Geothermal Resource Assessment and Reservoir Engineering, Larderello, Italy (Sept. 12-16, 1977), 256-298.

11. Sestini, G.: "Superheating of Geothermal Steam," Geothermics, Special Issue 2 (1970).

12. Celati, R., Squarci, P., Stefani, G.C., and Taffi, L.: "Study of Water Levels in Larderello Region Geothermal Wells for Reconstruction of Reservoir Pressure Trend," Simposio internacional sobre Energia Geotermica en America Latina, IILA-INDE (1976).

13. Celati, R., Noto, P., Panichi, C., Squarci, P., and Taffi, L.: "Interactions between the Steam Reservoir and Surrounding Aquifers in the Larderello Geothermal Field," Geothermics, (1973) 2, 174-185.

14. Barelli, A., Manetti, G., Celati, R., and Neri, G.: "Build-Up and Backpressure Tests on Italian Geothermal Wells," Proc., Second UN Symposium on the Development and Use of Geothermal Resources, San Francisco, Ca., (May 20-29, 1975), 1537-1546.

15. Celati, R., Squarci, P., Neri, G., and Perusini, P.: "An Attempt to Correlate kH Distribution with Geological Structure of Larderello Geothermal Field," Proc., First Stanford Workshop on Geothermal Reservoir Engineering, Stanford, Ca., (1975), 37-41.

16. Atkinson, P., Celati, R., Marconcini, R., Miller, F., and Neri., G.: "Analysis of Reservoir Pressure and Decline Curves in Serrazzano Zone - Larderello Geothermal Field," Proc., Larderello Workshop on Geothermal Resource Assessment and Reservoir Engineering, Larderello, Italy, (Sept. 12-16, 1977), 208-232.

17. Weres, O., Tsao, K., and Wood, B.: "Resource, Technology and Environment at The Geysers," Lawrence Berkeley Laboratory Report LBL-5231, (July 1977).

18. Weres, O.: "A Model of the Serrazzano Zone," Proc., Third Stanford Workshop on Geothermal Reservoir Engineering, Stanford, Ca., (1977), 214-219.

19. Weres, O., and Schroeder, R.C., Documentation for Program OGRE, Lawrence Berkeley Laboratory Report LBL-7060, Berkeley, CA (June 1978).